SAND95-0129C
Frontiers in Industrial Process Tomography, October 29 - November 3, 1995, San Luis Obispo, California

GAMMA DENSITOMETRY TOMOGRAPHY OF GAS HOLDUP SPATIAL DISTRIBUTION IN INDUSTRIAL SCALE BUBBLE COLUMNS

K. A. Shollenberger[1], J. R. Torczynski[1], D. R. Adkins[1], T. J. O'Hern[1], and N. B Jackson[2]
[1]Engineering Sciences Center and [2]Advanced Energy Technology Center
Sandia National Laboratories
Albuquerque, New Mexico 87185

ABSTRACT

Gamma-densitometry tomography (GDT) experiments have been performed to measure gas holdup spatial variations in two bubble columns: a 0.19 m inside diameter Lucite column and a 0.48 m inside diameter stainless steel vessel. Air and water were used for the measurements. Horizontal scans at one vertical position in each column were made for several air flow rates. An axisymmetric tomographic reconstruction algorithm based on the Abel transform has been used to calculate the time averaged gas holdup radial variation. Integration of these profiles over the column cross section has yielded area-averaged gas holdup results, which have been compared with volume-averaged gas holdups determined from differential pressure measurements and from the rise in the air/water interface during gas flow. The results agree reasonably well.

INTRODUCTION

Bubble-column reactors are used extensively by chemical manufacturers to perform a wide variety of gas/liquid or gas/liquid/solid reactions such as oxidation, hydrogenation, chlorination, aerobic fermentation and coal liquefaction (Shah and Deckwer, 1983). Bubble-column reactors are generally tall, cylindrical vessels filled with liquid, sometimes laden with a solid catalyst,

through which a gas is injected using a sparger at or near the bottom. The gas reacts with the liquid or catalyst to form a desired product, either a gas or a liquid, that is continuously removed from the vessel. Pressures and temperatures are controlled during the reaction to optimize product distribution. One of the main benefits of slurry-phase bubble-column reactors used in catalytic reactions is the ability of the liquid phase to provide an efficient heat sink for highly exothermic reactions. Under industrial conditions, the pressure, temperature, inlet gas velocity, and column diameter may be increased, to maximize total product production rates. The effects of increasing these parameters on the multiphase flow phenomenology must be considered when attempting to scale laboratory reactors to industrial sizes and operating conditions. Development and application of noninvasive tomographic diagnostics capable of measuring gas holdup (ratio of local gas volume to total volume) spatial distributions in full-scale reactors will greatly facilitate current efforts to predict reactor performance.

Gamma densitometry has been applied for measurement of local density in multiphase flows for some time (e.g., Petrick and Swanson, 1958; Swift et al., 1978; Chan and Banerjee, 1981). Standard gamma densitometry measures gamma attenuation integrated along a path through the medium, and thus lacks spatial resolution. However, spatially resolved measurements can be made by applying tomographic reconstruction algorithms to the results of measurements along many different paths. Although gamma-densitometry tomography (GDT) can measure spatially resolved gas holdup in a gas/liquid flow, neither instantaneous gas holdup nor bubble size distributions can be measured due to the time required for data acquisition. Several groups have applied GDT to measure multiphase flows. DeVuono et al. (1980) demonstrated a GDT system for air/water measurements at gas holdups up to 46%. MacCuaig et al. (1985) used GDT to examine a miniature fluidized bed (51 mm diameter), with a filtered back-projection algorithm employed to

reconstruct a two-dimensional image of the flow field. Brown et al. (1993) discuss design of a GDT system for measurements of flow in porous media, including a careful examination of error sources and accuracy.

Kumar et al. (1995) recently published an excellent overview of the GDT technique as applied to multiphase flow measurements. They include design considerations and results for their system applied to a bubble column, and carefully discuss possible error sources and means to mitigate them.

EXPERIMENTAL SETUP

Gamma Tomography System

A GDT system has been assembled for use in multiphase flow measurements, with the ultimate goal of fielding an industrial-scale system for measurements in operating process equipment and chemical reactors. The GDT system (see Figure 1) consists of a 5-Curie ^{137}Cs gamma source, a sodium iodide (NaI) with thallium (Tl) activator scintillation detector, a photomultiplier tube, a pre-amplifier, a single-channel analyzer, a computer-controlled traverse, and data acquisition/ analysis hardware and software. Such a GDT system is well suited to industrial measurements: the gamma photon energy for ^{137}Cs (661.6 keV) is appropriate for measurements through steel or concrete (Gilboy et al., 1982) for vessels up to a meter in diameter (Morton and Simons, 1995), and the thirty-year half-life is convenient.

The GDT system can accommodate apertures of different diameters on both the source (D_s) and detector (D_d). Four combinations have been examined where D_s and D_d were either 3.175 mm or 6.35 mm. The detector, positioned opposite the source, is water-cooled with active control to provide temperature stability and thus minimize thermal drift of the electronics. The source and the detector are both lead-shielded and mounted on opposite arms of a heavy-duty two-axis

traverse. The traverse source-detector separation is sufficient to accommodate vessels with diameters up to 0.66 m, and there is approximately 0.6 m of travel along each axis. The source and the detector are translated simultaneously to locations where data is to be acquired, with automatic system shutdown if a source-detector misalignment greater than 1 mm is detected. Operation of this system is fully automated: the operator selects a scan direction (vertical or horizontal), a step size (distance from one ray to the next), and either a dwell time (time to collect data for each ray) or total number of counts to collect, and the computer controls all subsequent actions. The data acquisition and analysis package is used to convert the individual photon signals to a count rate that can be used to determine gamma attenuation.

Bubble Columns

An air/water bubble column has been assembled for optical validation of the GDT technique under dynamic conditions (see Figure 2). The Lucite bubble column has a 0.19 m inner diameter and is 1.8 m tall. The column is initially filled with water to a height of 6 diameters. Gas is then introduced through one of several interchangeable distributors (spargers) located at the base of the column. The change in liquid level is monitored using a high-speed video camera to determine the average gas holdup in the air/water column over a range of gas flow rates, or superficial gas velocities (the gas volume flow rate divided by the column cross sectional area). During steady air flow, the volume-averaged gas holdup can be determined according to $\varepsilon_G = \Delta H / (H_0+\Delta H)$, where H_0 is the height of the water with no air flow and ΔH is the change in height during air flow. To date, gas holdups up to 40% have been observed for superficial velocities up to 0.35 m/s.

A second bubble column, capable of operating under industrially relevant conditions, has also been assembled and is shown schematically in Figure 3. The column is a stainless steel vessel with an inside diameter of 0.48 m, 1.27 cm thick walls, a height of 3 m and visual and instrumen-

tation ports at 6 axial locations separated by 0.46 m. This column is typically operated with an initial liquid height of 4 diameters. The vessel can be run at temperatures up to 200 °C and pressures up to 6.8 atm. The instrumentation ports are currently being used to measure the axial pressure gradient (*dP/dz*) along the column. These measurements are used to calculate gas holdups for comparison to GDT results using the following equation

$$\varepsilon_G = \frac{\rho_L - \rho}{\rho_L - \rho_G}, \qquad \rho = \frac{-dP/dz}{g}$$

where ρ_L, ρ_G, and ρ are the densities of the gas, liquid, and two phase mixture, respectively, g is the gravitational constant. The above equation assumes that the flow is steady and that the shear stress at the walls is negligible. To date, gas holdups up to 40% have been observed for superficial gas velocities up to 0.40 m/s at atmospheric conditions.

TOMOGRAPHIC RECONSTRUCTION

GDT reconstructions of gas holdup spatial distribution rely on measurements of the extinction of a gamma beam of known intensity I_0 (count rate, counts per second) along a ray (straight line) passing through an attenuating medium. If an intensity I is measured when the beam passes through a portion of the attenuating medium, the intensity change is related to the attenuation coefficient μ of the medium by

$$\frac{I}{I_0} = \exp[-\int \mu ds]$$

where s is the distance along the portion of the ray intersecting the attenuating medium. The attenuation A is given by

$$A = -\ln\left[I/I_0\right] = \int \mu ds$$

Thus, the attenuation A and the attenuation coefficient μ are linearly related. Additionally, the spatial variation of μ can be tomographically reconstructed if the spatial variation of A is known. It is the task of tomographic reconstruction algorithms to determine the spatial variation of the attenuation coefficient μ based on the attenuation measurements, which are line integrals of μ. Under axisymmetric conditions, only a single projection is required, and the reconstruction is performed using the Abel transform (cf. Vest, 1985). If $f(r, R)$ is a function of radial position that is nonzero only within a circle of radius R, then its Abel transform is

$$\phi(x, R) = 2 \int_0^{\sqrt{R^2 - x^2}} f(\sqrt{x^2 + y^2}, R)\, dy = 2 \int_x^R \frac{f(r, R) r}{\sqrt{r^2 - x^2}}\, dr$$

which is merely the line integral along the ray in the y direction at x. This relation can be inverted to yield f in terms of ϕ using the Abel inversion formula

$$f(r, R) = -\frac{1}{\pi} \int_r^R \frac{(d\phi/dx)}{\sqrt{x^2 - r^2}}\, dx$$

Note that for GDT, ϕ corresponds to A and f corresponds to μ. A quantity that arises naturally in tomography considerations is ψ, the "ray averaged" value of f, given by

$$\psi(x, R) = \frac{\phi(x, R)}{2\sqrt{R^2 - x^2}}$$

which, as indicated, is just the line integral of f along the ray at x divided by the path length. The functions f and ψ have a remarkable property that is useful to tomographic reconstruction algorithms: if one function is an even polynomial, then the other function is also an even polynomial of the same degree. For the following representations of f and ψ,

$$f(r, R) = \sum_{m=0}^{N} a_m (r/R)^{2m}, \quad \psi(x, R) = \sum_{n=0}^{N} b_n (x/R)^{2n}$$

SAND95-0129C
Frontiers in Industrial Process Tomography, October 29 - November 3, 1995, San Luis Obispo, California

GAMMA DENSITOMETRY TOMOGRAPHY OF GAS HOLDUP SPATIAL DISTRIBUTION IN INDUSTRIAL SCALE BUBBLE COLUMNS

K. A. Shollenberger[1], J. R. Torczynski[1], D. R. Adkins[1], T. J. O'Hern[1], and N. B Jackson[2]
[1]Engineering Sciences Center and [2]Advanced Energy Technology Center
Sandia National Laboratories
Albuquerque, New Mexico 87185

ABSTRACT

Gamma-densitometry tomography (GDT) experiments have been performed to measure gas holdup spatial variations in two bubble columns: a 0.19 m inside diameter Lucite column and a 0.48 m inside diameter stainless steel vessel. Air and water were used for the measurements. Horizontal scans at one vertical position in each column were made for several air flow rates. An axisymmetric tomographic reconstruction algorithm based on the Abel transform has been used to calculate the time averaged gas holdup radial variation. Integration of these profiles over the column cross section has yielded area-averaged gas holdup results, which have been compared with volume-averaged gas holdups determined from differential pressure measurements and from the rise in the air/water interface during gas flow. The results agree reasonably well.

INTRODUCTION

Bubble-column reactors are used extensively by chemical manufacturers to perform a wide variety of gas/liquid or gas/liquid/solid reactions such as oxidation, hydrogenation, chlorination, aerobic fermentation and coal liquefaction (Shah and Deckwer, 1983). Bubble-column reactors are generally tall, cylindrical vessels filled with liquid, sometimes laden with a solid catalyst,

through which a gas is injected using a sparger at or near the bottom. The gas reacts with the liquid or catalyst to form a desired product, either a gas or a liquid, that is continuously removed from the vessel. Pressures and temperatures are controlled during the reaction to optimize product distribution. One of the main benefits of slurry-phase bubble-column reactors used in catalytic reactions is the ability of the liquid phase to provide an efficient heat sink for highly exothermic reactions. Under industrial conditions, the pressure, temperature, inlet gas velocity, and column diameter may be increased, to maximize total product production rates. The effects of increasing these parameters on the multiphase flow phenomenology must be considered when attempting to scale laboratory reactors to industrial sizes and operating conditions. Development and application of noninvasive tomographic diagnostics capable of measuring gas holdup (ratio of local gas volume to total volume) spatial distributions in full-scale reactors will greatly facilitate current efforts to predict reactor performance.

Gamma densitometry has been applied for measurement of local density in multiphase flows for some time (e.g., Petrick and Swanson, 1958; Swift et al., 1978; Chan and Banerjee, 1981). Standard gamma densitometry measures gamma attenuation integrated along a path through the medium, and thus lacks spatial resolution. However, spatially resolved measurements can be made by applying tomographic reconstruction algorithms to the results of measurements along many different paths. Although gamma-densitometry tomography (GDT) can measure spatially resolved gas holdup in a gas/liquid flow, neither instantaneous gas holdup nor bubble size distributions can be measured due to the time required for data acquisition. Several groups have applied GDT to measure multiphase flows. DeVuono et al. (1980) demonstrated a GDT system for air/water measurements at gas holdups up to 46%. MacCuaig et al. (1985) used GDT to examine a miniature fluidized bed (51 mm diameter), with a filtered back-projection algorithm employed to

reconstruct a two-dimensional image of the flow field. Brown et al. (1993) discuss design of a GDT system for measurements of flow in porous media, including a careful examination of error sources and accuracy.

Kumar et al. (1995) recently published an excellent overview of the GDT technique as applied to multiphase flow measurements. They include design considerations and results for their system applied to a bubble column, and carefully discuss possible error sources and means to mitigate them.

EXPERIMENTAL SETUP

Gamma Tomography System

A GDT system has been assembled for use in multiphase flow measurements, with the ultimate goal of fielding an industrial-scale system for measurements in operating process equipment and chemical reactors. The GDT system (see Figure 1) consists of a 5-Curie ^{137}Cs gamma source, a sodium iodide (NaI) with thallium (Tl) activator scintillation detector, a photomultiplier tube, a pre-amplifier, a single-channel analyzer, a computer-controlled traverse, and data acquisition/ analysis hardware and software. Such a GDT system is well suited to industrial measurements: the gamma photon energy for ^{137}Cs (661.6 keV) is appropriate for measurements through steel or concrete (Gilboy et al., 1982) for vessels up to a meter in diameter (Morton and Simons, 1995), and the thirty-year half-life is convenient.

The GDT system can accommodate apertures of different diameters on both the source (D_s) and detector (D_d). Four combinations have been examined where D_s and D_d were either 3.175 mm or 6.35 mm. The detector, positioned opposite the source, is water-cooled with active control to provide temperature stability and thus minimize thermal drift of the electronics. The source and the detector are both lead-shielded and mounted on opposite arms of a heavy-duty two-axis

traverse. The traverse source-detector separation is sufficient to accommodate vessels with diameters up to 0.66 m, and there is approximately 0.6 m of travel along each axis. The source and the detector are translated simultaneously to locations where data is to be acquired, with automatic system shutdown if a source-detector misalignment greater than 1 mm is detected. Operation of this system is fully automated: the operator selects a scan direction (vertical or horizontal), a step size (distance from one ray to the next), and either a dwell time (time to collect data for each ray) or total number of counts to collect, and the computer controls all subsequent actions. The data acquisition and analysis package is used to convert the individual photon signals to a count rate that can be used to determine gamma attenuation.

Bubble Columns

An air/water bubble column has been assembled for optical validation of the GDT technique under dynamic conditions (see Figure 2). The Lucite bubble column has a 0.19 m inner diameter and is 1.8 m tall. The column is initially filled with water to a height of 6 diameters. Gas is then introduced through one of several interchangeable distributors (spargers) located at the base of the column. The change in liquid level is monitored using a high-speed video camera to determine the average gas holdup in the air/water column over a range of gas flow rates, or superficial gas velocities (the gas volume flow rate divided by the column cross sectional area). During steady air flow, the volume-averaged gas holdup can be determined according to $\varepsilon_G = \Delta H / (H_0+\Delta H)$, where H_0 is the height of the water with no air flow and ΔH is the change in height during air flow. To date, gas holdups up to 40% have been observed for superficial velocities up to 0.35 m/s.

A second bubble column, capable of operating under industrially relevant conditions, has also been assembled and is shown schematically in Figure 3. The column is a stainless steel vessel with an inside diameter of 0.48 m, 1.27 cm thick walls, a height of 3 m and visual and instrumen-

tation ports at 6 axial locations separated by 0.46 m. This column is typically operated with an initial liquid height of 4 diameters. The vessel can be run at temperatures up to 200 °C and pressures up to 6.8 atm. The instrumentation ports are currently being used to measure the axial pressure gradient (*dP/dz*) along the column. These measurements are used to calculate gas holdups for comparison to GDT results using the following equation

$$\varepsilon_G = \frac{\rho_L - \rho}{\rho_L - \rho_G}, \qquad \rho = \frac{-dP/dz}{g}$$

where ρ_L, ρ_G, and ρ are the densities of the gas, liquid, and two phase mixture, respectively, g is the gravitational constant. The above equation assumes that the flow is steady and that the shear stress at the walls is negligible. To date, gas holdups up to 40% have been observed for superficial gas velocities up to 0.40 m/s at atmospheric conditions.

TOMOGRAPHIC RECONSTRUCTION

GDT reconstructions of gas holdup spatial distribution rely on measurements of the extinction of a gamma beam of known intensity I_0 (count rate, counts per second) along a ray (straight line) passing through an attenuating medium. If an intensity I is measured when the beam passes through a portion of the attenuating medium, the intensity change is related to the attenuation coefficient μ of the medium by

$$\frac{I}{I_0} = \exp[-\int \mu ds]$$

where s is the distance along the portion of the ray intersecting the attenuating medium. The attenuation A is given by

$$A = -\ln\left[I/I_0\right] = \int \mu ds$$

Thus, the attenuation A and the attenuation coefficient μ are linearly related. Additionally, the spatial variation of μ can be tomographically reconstructed if the spatial variation of A is known. It is the task of tomographic reconstruction algorithms to determine the spatial variation of the attenuation coefficient μ based on the attenuation measurements, which are line integrals of μ. Under axisymmetric conditions, only a single projection is required, and the reconstruction is performed using the Abel transform (cf. Vest, 1985). If $f(r, R)$ is a function of radial position that is nonzero only within a circle of radius R, then its Abel transform is

$$\phi(x, R) = 2 \int_0^{\sqrt{R^2 - x^2}} f(\sqrt{x^2 + y^2}, R)\, dy = 2 \int_x^R \frac{f(r, R) r}{\sqrt{r^2 - x^2}}\, dr$$

which is merely the line integral along the ray in the y direction at x. This relation can be inverted to yield f in terms of ϕ using the Abel inversion formula

$$f(r, R) = -\frac{1}{\pi} \int_r^R \frac{(d\phi/dx)}{\sqrt{x^2 - r^2}}\, dx$$

Note that for GDT, ϕ corresponds to A and f corresponds to μ. A quantity that arises naturally in tomography considerations is ψ, the "ray averaged" value of f, given by

$$\psi(x, R) = \frac{\phi(x, R)}{2\sqrt{R^2 - x^2}}$$

which, as indicated, is just the line integral of f along the ray at x divided by the path length. The functions f and ψ have a remarkable property that is useful to tomographic reconstruction algorithms: if one function is an even polynomial, then the other function is also an even polynomial of the same degree. For the following representations of f and ψ,

$$f(r, R) = \sum_{m=0}^{N} a_m (r/R)^{2m}, \quad \psi(x, R) = \sum_{n=0}^{N} b_n (x/R)^{2n}$$

the following "reconstruction" relations can be derived with a bit of effort:

$$a_m = \sum_{n=0}^{N} c_{mn} b_n \quad \text{and} \quad b_n = \sum_{m=0}^{N} d_{nm} a_m$$

where (in terms of binomial coefficients)

$$c_{mn} = \begin{cases} -\left[\dfrac{2m+1}{2^{2n}(2n-2m-1)}\right]\begin{pmatrix} 2n-2m \\ n-m \end{pmatrix}\begin{pmatrix} 2m \\ m \end{pmatrix}, & m \le n \\ 0, & m > n \end{cases}$$

$$d_{nm} = \begin{cases} \left(\dfrac{2^{2n}}{2m+1}\right)\begin{pmatrix} 2m-2n \\ m-n \end{pmatrix}\Big/\begin{pmatrix} 2m \\ m \end{pmatrix}, & n \le m \\ 0, & (n > m \end{cases}$$

Tomographic reconstruction of an axisymmetric gas holdup spatial distribution proceeds in the following manner: (a) measure the ray averaged gas holdups ψ_i on a set of rays x_i, (b) fit the (x_i, ψ_i) with even powers of x/R to find the b_n, and (c) use the c_{mn} to determine the a_m and the gas holdup radial variation f.

The ψ_i values (ray averaged gas holdup data) were determined according to the relation

$$\psi_i = \frac{A_i^{\text{full}} - A_i^{\text{flow}}}{A_i^{\text{full}} - A_i^{\text{empty}}}$$

where "full" denotes the value when the column is completely full of water (zero gas holdup), "empty" denotes the value when the column is completely empty of water (unity gas holdup), and "flow" denotes the value when air is flowing through a filled column. Thus, the technique is self-calibrated by using the full and empty signals at each location to calculate the gas holdup.

UNCERTAINTY ANALYSIS

There are several sources of uncertainty that must be accounted for and minimized when making gamma-densitometry measurements. In general, and for our system and application, they can be listed as follows:

1. System drift.
2. Nonlinear detector response due to dead time.
3. Compton scattering effects.
4. Background noise.
5. Statistical uncertainty in photon counts.
6. Uncertainties due to flow variations.
7. Image reconstruction errors.

As noted in the Experimental Setup section the detector is water-cooled to provide temperature stability which minimizes drifts in the observed count rates. Furthermore, full and empty scans of the column are taken periodically to ensure continual calibration of the method.

Scintillation detector count rate (dead time) effects are discussed in detail by several authors (e.g. Reda et al.,1981; Rózsa, 1989). The detector converts each individual gamma photon into a light pulse, which is detected using a photomultiplier tube. The light energy emitted rises sharply as a function of time until it reaches a maximum and then begins to decay exponentially. The system thus has an inherent time scale τ and measurements at rates comparable to or exceeding $1/\tau$ will not directly yield accurate count rates. Reda et al. (1981) provide measurements indicating τ = 3-5 μs, where the observed nonlinear response is fitted to the following model:

$$I = \frac{I_{obs}}{1 - \tau I_{obs}}$$

I_{obs} is the observed or measured intensity and I is the actual intensity in counts/s. For our range of conditions, τ has been estimated by first obtaining both "full" and "empty" scans of the column at known locations. The ratio of the "full" and "empty" count rate at each location is then compared to the expected attenuation predicted using the exponential decay law, the known path length

through the water and the attenuation coefficient for water. Finally, the nonlinear model given above by Reda et.al. (1981) is used to correct for the deviation between the expected and observed values. τ was measured to be 1.94 μs for our GDT system operated on the 0.48 m stainless steel column. Figures 4 (a) and (b) show the effect of τ on our GDT measurements in the large column for two different sets of collimators (i.e. different incident radiation intensity levels I_0). For this data set, only the points in figure (b) that were taken outside of the column (i.e. through air alone) begin to lie in the nonlinear response region of the detector (i.e. where the solid line departs from the dashed line as I increases). Thus, for the current set of operating conditions, measured intensities or count rates do not need to be corrected using τ to yield accurate values.

The primary mode of attenuation of the photons emitted from a ^{137}Cs source at an energy of 661.6 keV is Compton scattering (Lapp and Andrews, 1972). For these interactions, an incident photon is absorbed by an electron, but only a portion of the photon's energy is transferred to the ejected electron. A new photon of lower energy than the original is created that in general will not have the same direction as the original. This process occurs both in the vessel and in the detector. Collimation is used at the detector to minimize the number of photons scattered at low angles from entering the detector. In addition, a spectrum analysis of the energy levels of the detected photons is used to discriminate against Compton scattered photons that do manage to enter the crystal (see Figure 5). An energy filter or "window" is set in the data acquisition electronics around the ^{137}Cs peak to reduce the influence of scattered photons on the measured count rate.

Also noticeable in Figure 5 is the presence of "background noise," due to electrical noise and background radiation, that is recorded even when the source is closed. This represents a systematic bias in the signal that will increase all count rates by approximately the same amount in the

linear response region of the detector. For our system, the background noise is approximately 2.5 counts/s, which results in an uncertainty of less than 0.7%.

Statistical uncertainty in the photon count rate arises from the normal fluctuations in the arrival of photons with time, which can be well approximated by the Poisson distribution (Lapp and Andrews, 1972). From this distribution, the statistical deviation in any measurement of photons emitted by a source of gamma radiation can be shown to be equal to the square root of the total number of counts N observed. In order to demonstrate our ability to measure a known length L of water using changes in intensity to the accuracy specified by the above statistics, the column was scanned both full (I) and empty (I_0), and the following equation was used to calculate L:

$$L = \frac{-1}{\mu} \ln\left(\frac{I}{I_0}\right)$$

If the error in the measurement of the time period is assumed negligible, then the uncertainty in the measurement of the fluid length can be approximated using Taylor's theorem

$$|dL| = \left[\left(dI \frac{\partial L}{\partial I}\right)^2 + \left(dI_0 \frac{\partial L}{\partial I_0}\right)^2\right]^{1/2}$$

substituting in the above definition for L

$$|dL| = \left[\left(\frac{-1}{\mu} \frac{dI}{I}\right)^2 + \left(\frac{1}{\mu} \frac{dI_0}{I_0}\right)^2\right]^{1/2}$$

substituting in $dI/I = 1/\sqrt{N}$ and dividing by L

$$\frac{|dL|}{L} = \frac{1}{\mu L}\left(\frac{1}{N} + \frac{1}{N_0}\right)^{1/2}$$

Figure 6 shows results for two sets of collimators, 3.175 mm and 6.35 mm in diameter, for which the total number of counts were 2,000 and 20,000, corresponding to average predicted uncertainties of 1.52% and 0.48% for the locations used, respectively. The measured errors were 0.73% and

0.45%, demonstrating that the path length can be measured accurately through a known medium and that other sources of error, such as nonlinear detector response, noise, and uncertainties due to dimensional inaccuracies, were negligible.

Up to this point, the errors discussed are all of importance for a steady-state measurement. New uncertainties are introduced as a result of the unsteady flow pattern in the bubble column: a continuous fluctuation of gas in and out of the domain being measured. To obtain a good average of the gas content along any ray, one must ideally sample at a rate of at least two measurements per cycle for the maximum frequency present over a significant number of cycles according to the Nyquist theory. Furthermore, according to the equations given above for calculating gas holdup, the average of the natural log of the count rate is needed. However, the average count rate is what is actually measured and its natural log is taken in the analysis. This leads to a systematic overestimation or bias of the desired value that will be more significant for large periodic fluctuations in the flow. One way of dealing with this problem, as outlined by previous authors (Kumar, et al., 1995, Pan and Hewitt, 1995), is to obtain enough counts in a time period that is assumed to be a fraction of the time scale for the flow, take the natural logarithm of many of these values and average them together. If 1000 counts per sample are collected, the same as in Kumar's study, for our current system design we can at best reduce our sample times to 2 to 3 seconds near the center of the vessel. The time scales in the flow do not appear to be nearly this long. Thus, for a large vessel, sampling periods will generally have to be longer than the inherent time scales of the bubble column. However, if deviations of gas holdup from the mean along a ray of increasing length become less likely, the uncertainty will become negligible. Methods for obtaining a quantitative estimate of this uncertainty are currently being pursued.

Finally, the uncertainty in the calculated gas holdup along a ray can be estimated from the uncertainties in the measured intensities collected. Using the equations for A and ψ_i from the Tomographic Reconstruction section, the ray averaged gas holdup can be written as

$$\psi_i = \frac{\ln(I_i^{full}) - \ln(I_i^{flow})}{\ln(I_i^{full}) - \ln(I_i^{empty})} = \frac{\ln(I_i^{full}/I_i^{flow})}{\ln(I_i^{full}/I_i^{empty})}$$

where I_i^{flow},I_i^{full} and I_i^{empty} are the count rates measured with a bubbly flow, water and air in the vessel, respectively. The uncertainty in the gas holdup measurement is again estimated using Taylor's theorem

$$|d\psi_i| = \left[\left(dI_i^{flow}\ \frac{\partial\psi_i}{\partial I_i^{flow}}\right)^2 + \left(dI_i^{full}\ \frac{\partial\psi_i}{\partial I_i^{full}}\right)^2 + \left(dI_i^{empty}\ \frac{\partial\psi_i}{\partial I_i^{empty}}\right)^2\right]^{1/2}$$

substituting in the equation for ψ_i, $dI/I = 1/\sqrt{N}$ where N is the total number of counts observed for all three intensity measurements and $\mu L = \ln(I_i^{empty}/I_i^{full})$

$$\frac{|d\psi_i|}{\psi_i} = \frac{1}{\mu L\, \psi_i}\sqrt{\frac{2\,(\psi_i^2 - \psi_i + 1)}{N}}$$

It is found that the uncertainty is a function of the total number of counts (N), the contrast μL between the gas and liquid intensities, and the ray averaged gas holdup being measured. This relationship is shown graphically in Figure 7 for the 0.48 m inside diameter stainless steel column where a total of 20,000 counts (N) are taken at each location. For this column, the contrast in the central region of the column (inner 0.4 m) is sufficient to make measurements of gas holdups greater than 8% with less than $\pm$ 0.4% deviation in magnitude.

This error estimate, again, is for the ray-averaged gas holdup measurement. For the reconstruction process, the data set is initially curve-fitted to a polynomial. Conceptually, the curve fit has two possible sources of error: (1) the data may not be perfectly matched by the chosen func-

tional form and (2) noise in the data will also result in error in the fit. The reconstruction itself further affects the accuracy of the gas holdup measurement because it is a linear transform: the error is transformed in the same way as the original function. If the averaged gas holdup profile is a smooth function as assumed by the reconstruction process, a good fit should produce a better representation of the gas holdup profile than the original ray-averaged data. However, since the gas holdup near the walls is very difficult to predict due to the poor contrast in that region, large inaccuracies at this location could cause an increase in the error in the average gas holdup measurement. We are testing the accuracy of the average gas holdups obtained from reconstruction by comparing the computed gas holdups to values calculated using expanded height and differential pressure methods as outlined in the Experimental Setup section.

RESULTS

GDT results have been obtained for gas holdup spatial distributions in the 0.19 m air/water Lucite bubble column at several air flow rates. A bubble-cap sparger located 10 cm above the bottom of the column was employed, and the plane 0.57 m ($z/D = 3$) above the sparger was examined. Air flow rates of 0, 25, 100 and 200 liters/min were examined, corresponding to gas superficial velocities of 0, 0.0147, 0.0588, and 0.1176 m/s, where the zero flow case has zero gas holdup. At each flow rate, a series of intensities I_i was measured for a series of rays x_i, and the corresponding attenuations A_i were determined by taking the logarithm. For each scan, gamma rays were counted for 5 seconds at each of 218 rays, which were 1 mm apart along the horizontal direction. The collimators on both the source and the detector were 3.175 mm in diameter.

Figure 8 shows the attenuation data scatter and the curve fit used in the axisymmetric tomography to determine the radial variation in gas holdup. A fourth-order polynomial with even powers of horizontal position was used to fit the ray-averaged attenuation coefficient. For each flow, the

reconstructed attenuation profile based on the ray-averaged gas holdup data, the "full" profile, and the "empty" profile are shown. Figure 9 shows the GDT measured gas holdup as a function of radial location in the column, indicating (for this sparger) the highest gas holdup in the center of the column, falling smoothly to zero at the wall. This trend is in accord with the results of many other investigators (Shah and Deckwer, 1983). Volume-averaged gas holdups for the entire tank were obtained using level-rise measurements and were (for increasing superficial gas velocity) 2.0%, 6.6% and 10.2% which compare reasonably to the 2.4%, 8.2% and 12.6% values obtained from averaging GDT results over the profile. Here, a volume-averaged measurement is being compared to a planar measurement, so exact agreement is not expected.

GDT results have also been obtained for gas holdup spatial distributions in the 0.48 m stainless steel bubble column using air/water at atmospheric conditions. A ring-type sparger with upward facing holes with a diameter of approximately one-fourth the columns inner diameter was employed. The initial static liquid height was 1.93 m ($z/D = 4$) and the horizontal scans were made at a location of 0.96 m ($z/D = 2$) above the sparger. For each scan, incident intensities were observed for a total of 20,000 counts at each of 25 rays, which were 2.0 cm apart along the horizontal direction. The collimators on both the source and detector were 6.35 mm in diameter. Results for two air flow rates, gas superficial velocities of 0.088 and 0.39 m/s, are shown in Figure 10. A second order polynomial with even powers of horizontal position was used to curve fit the ray-averaged attenuation coefficient.

Comparing the results for the two columns in Figures 9 and 10, the profiles of gas holdup for the larger column, at the same flow rates, appear to be flatter. In addition, the gas holdup is no longer approaching zero at the walls. Volume-averaged gas holdups were also obtained for the 0.48 m column using differential pressures over the region of $z/D = 1.8$ to 2.7. They were 16% and

30% for the 0.088 and 0.39 m/s superficial gas velocity cases, respectively. These values compare fairly well with the 19% and 33% average gas holdups calculated by averaging the GDT reconstructions over the column cross section. The differences may be due to the difficulty in obtaining accurate gas holdup measurements near the wall of the vessel. Again, the differences may also be a result of significant variation in gas holdup over the volume-averaged region (i.e. over the one diameter length that the differential pressures were measured).

SUMMARY AND CONCLUSIONS

We have successfully demonstrated the ability to make accurate measurements of gas holdup spatial distributions using gamma densitometry tomography (GDT) in two air/water bubble columns, one of industrial scale. The reconstructed gas holdup profiles assumed axisymmetric flow and represented time-averaged data. Average gas holdups obtained from integrating the GDT results were in reasonable agreement with results from level-rise and differential pressure measurements for each bubble column. The control of sources of error was found to increase in importance for the larger vessel. In particular, the trade-off between obtaining statistical accuracy and resolving flow time scales becomes a critical issue. Further analysis will be conducted to determine the significance of this source of error for measurements of gas holdup in large vessels.

Several areas were identified for near term refinement of the GDT technique. To more accurately discretize detected gamma energies, a multichannel spectrum analyzer will be used to separate the unattenuated photons from the Compton scattered photons collected by the detector. GDT measurements will be extended to allow for better comparisons to the volume-averaged measurements of gas holdup obtained using the level-rise and differential pressure techniques. Finally, the reconstruction process will be extended to make non-axisymmetric reconstructions of gas holdup. Once these final improvements have been made to the GDT technique, a full parameter study

under industrially relevant conditions will be performed in the 0.48 m stainless steel bubble column reactor.

ACKNOWLEDGMENTS

The authors gratefully acknowledge the efforts Tom Grasser and John O'Hare of Sandia National Laboratories for their hard work assembling the GDT system and the bubble column. This work was performed at Sandia National Laboratories, supported by the U. S. Department of Energy under contract number DE-AC04-94AL85000. The support of DOE/Sandia Laboratory Directed Research and Development (LDRD) funds is gratefully acknowledged.

NOMENCLATURE

A	attenuation
c_{mn}	inverse Abel transform coefficients (nondimensional)
d_{mn}	forward Abel transform coefficients (nondimensional)
D	bubble column inside diameter (m)
D_d	detector aperture diameter (mm)
D_s	source aperture diameter (mm)
f	gas holdup radial variation (nondimensional)
g	gravitational constant (m/s)
ΔH	change in water depth with air flow (m)
H_0	water depth with no air flow (m)
I	gamma intensity (counts/s)
I_i^{empty}	gamma intensity for air alone in vessel (counts/s)
I_i^{flow}	gamma intensity for air/water flow in vessel (counts/s)

I_i^{full} gamma intensity for water alone in vessel (counts/s)

I_0 initial gamma intensity (counts/s)

I_{obs} observed or measured gamma intensity (counts/s)

j_G superficial gas velocity (m/s)

L path length through attenuating material (m)

N total number of photons counted

dP/dz axial differential pressure along column (Pa)

r radial position (m)

R bubble column inside radius (m)

x horizontal position (m)

z vertical or axial position (m)

ε_G gas holdup, gas volume divided by total volume (nondimensional)

μ attenuation coefficient (cm^{-1})

ρ density of gas/liquid mixture (kg/m^3)

ρ_G density of gas (kg/m^3)

ρ_L density of liquid (kg/m^3)

τ time scale for detector response (s)

ψ ray averaged gas holdup (nondimensional)

REFERENCES

Brown, G. O., Stone, M. L., and Gazin, J. E., 1993, Accuracy of gamma ray computerized tomography in porous media. *Water Resources Research* **29**:2, 479-486.

Bukur, D. B., Patel, S. A., and Matheo, R., 1987, Hydrodynamic studies in Fischer-Tropsch derived waxes in a bubble column. *Chem. Eng. Comm.* **60**, 63-78.

Chan, A. M. C. and Banerjee, S., 1981, Design aspects of gamma densitometers for void fraction measurements in small scale two-phase flows. *Nuclear Instruments and Methods* **190**, 135-148.

DeVuono, A. C., Schlosser, P. A., Kulacki, F. A., and Munshi, P., 1980, Design of an isotopic CT scanner for two phase flow measurement. *IEEE Trans. Nucl. Sci.* **NS-27**:1, 814-820.

Gilboy, W. B., Foster, J., and Folkard, M., 1982, A tomographic gamma-ray scanner for industrial applications. *Nuclear Instruments and Methods* **193**, 209-214.

Kumar, S. B., Moslemian, D., and Dudukovic, M. P., 1995, A γ-ray tomographic scanner for imaging voidage distribution in two-phase flow systems. *Flow Meas. Instrum.* **6**:1, 61-73.

Lapp, R. E. and Andrews, H. L., 1972, *Nuclear Radiation Physics*, Prentice-Hall, New Jersey.

MacCuaig, N., Seville, J. P. K., Gilboy, W. B., and Clift, R., 1985, Application of gamma-ray tomography to gas fluidized beds. *Applied Optics* **24**:23, 4083-4085.

Morton, E. J. and Simons, S. J. R., 1995, The physical basis of process tomography. *Frontiers in Industrial Process Tomography*, ed. Scott, D. M. and Williams, R. A., pp. 11-21. Engineering Foundation, New York.

Pan, Lei and Hewitt, G. F., 1995, Precise measurement of cross sectional phase fractions in three-phase flow using a dual-energy gamma densitometer. *ANS Proceedings, 1995 National Heat Transfer Conference* **8**. Portland, Oregon.

Petrick, M. and Swanson, B. S., 1958, Radiation attenuation method of measuring density of a two-phase flow. *Rev. Sci. Inst.* **29**:12, 1079-1085.

Reda, D. C., Hadley, G. R., and Turner, J. E. R., 1981, Application of the gamma-beam attenuation technique to the measurement of liquid saturation for two-phase flows in porous media. *Instrumentation in the Aerospace Industry* **27**, *Advances in Test Measurement* **18**, Part Two, *Proceedings of the 27th International Instrumentation Symposium*, K. E. Kissell, ed., pp. 553-568. Instrument Society of America, Research Triangle Park, NC.

Rózsa, S., 1989, *Nuclear Measurements in Industry*, Elsevier Science Publishing Co., New York.

Shah, Y. T. and Deckwer, W. D.,1983, Hydrodynamics of bubble columns. *Handbook of Fluids in Motion*, ed. Cheremisinoff, N. P. and Gupta, R., Ann Arbor Science Publishers, Michigan.

Swift. W. L., Dolan, F. X., and Runstadler, P. W., 1978, A scanning gamma ray attenuation system for void fraction measurements in two-phase flows. *Proceedings, Measurements in Polyphase Flows*, D. Stock, ed., American Society of Mechanical Engineers, pp. 25-35.

Vest, C. M., 1985, Tomography for properties of materials that bend rays: a tutorial. *Applied Optics* **24**:23, 4089-4094.

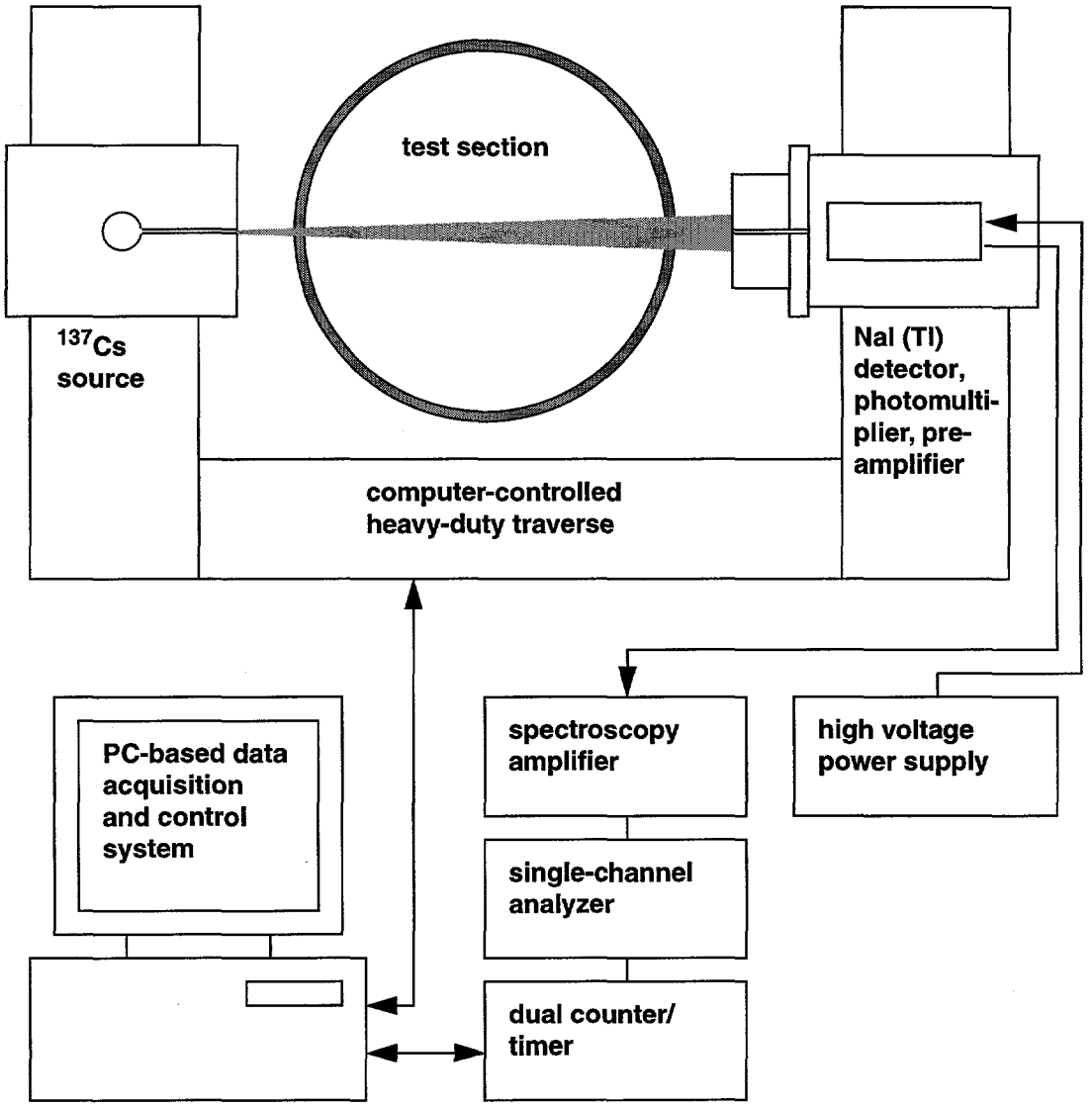

Figure 1. Schematic diagram of gamma-densitometry tomography (GDT) system setup.

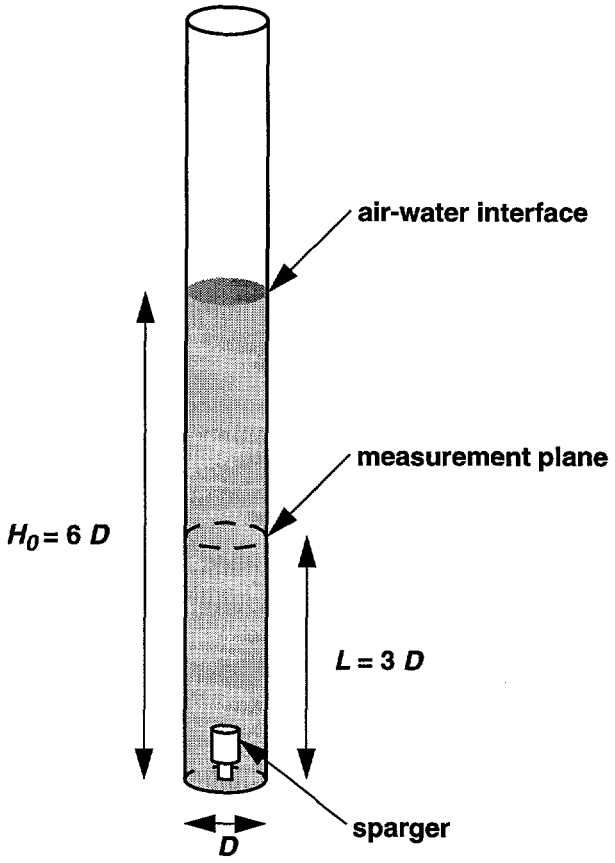

Figure 2. Schematic diagram of the 0.19 m ID Lucite air/water bubble column for GDT development and validation studies.

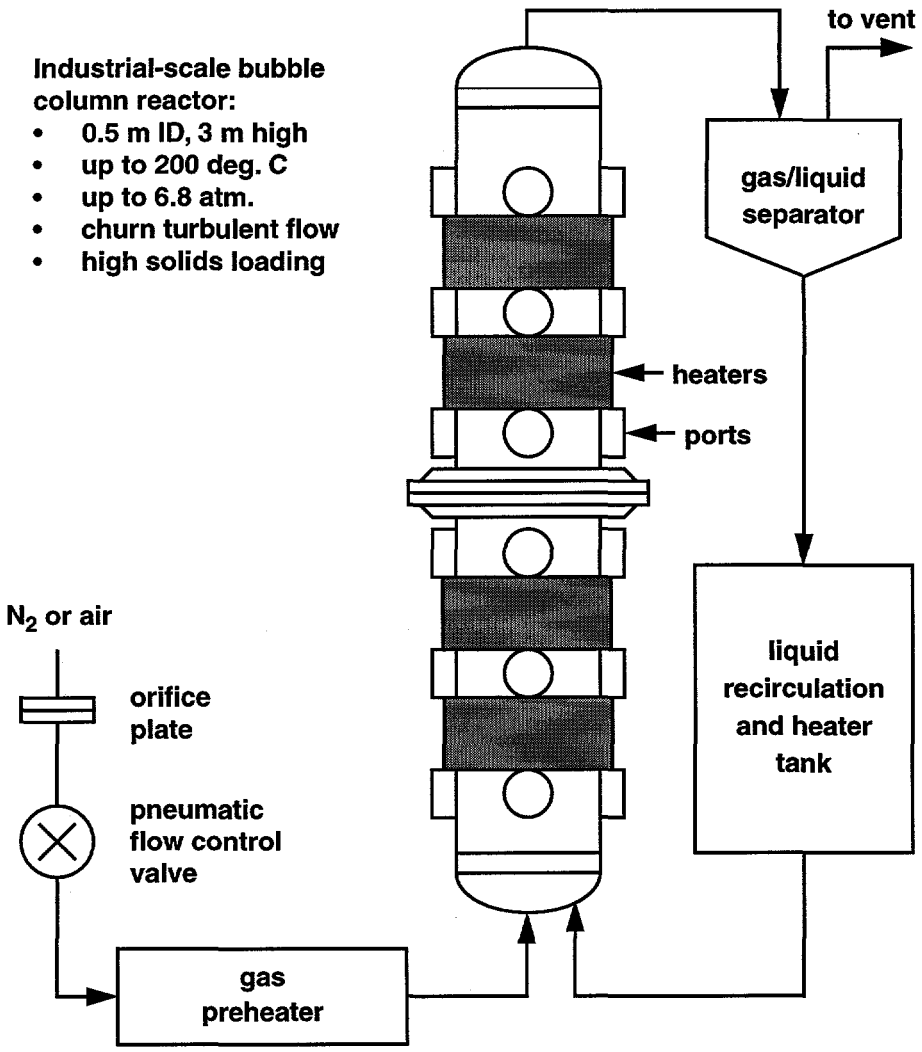

Figure 3. Schematic diagram of the 0.49 m ID stainless steel bubble column system for GDT measurements under industrial conditions.

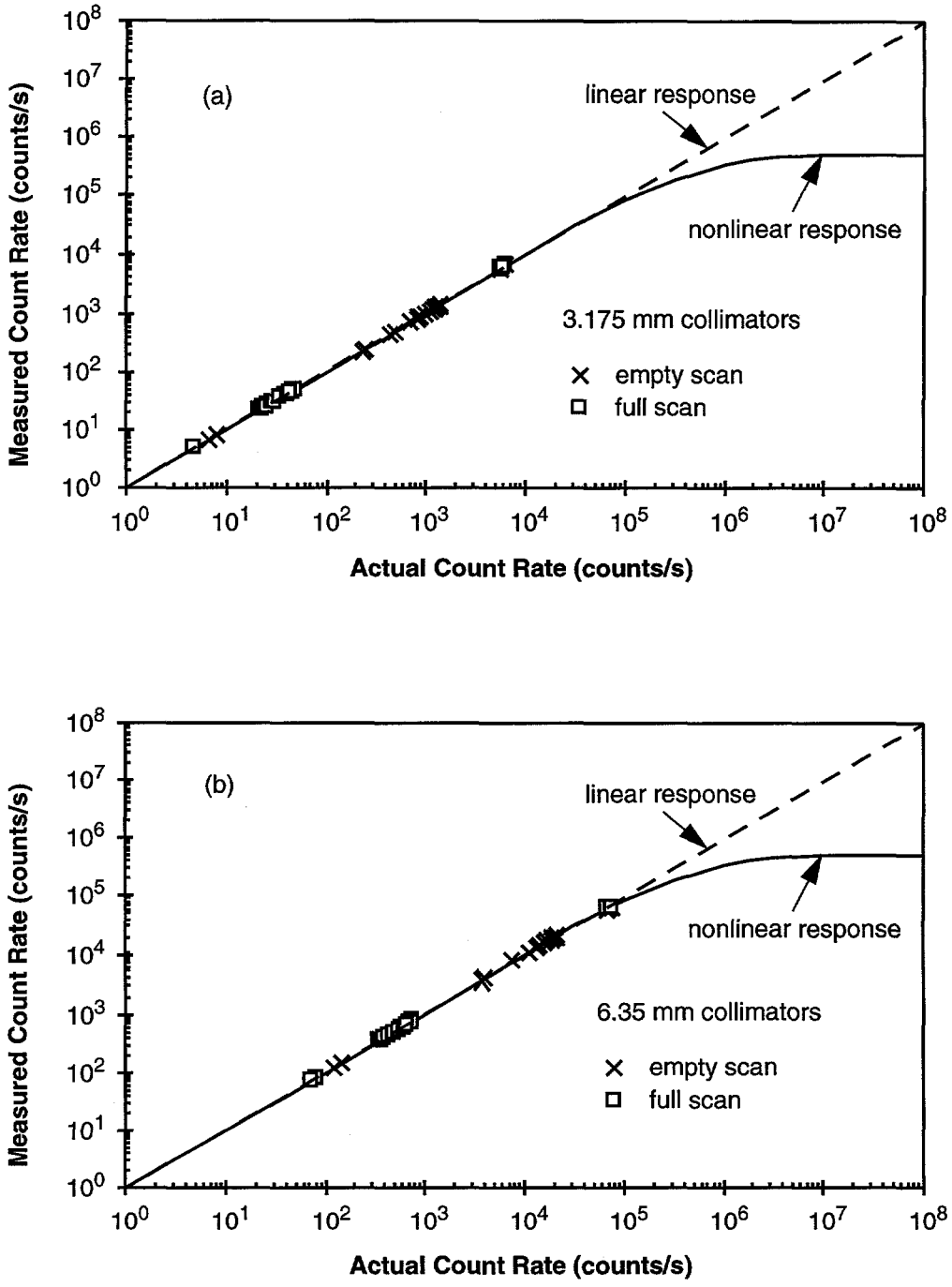

Figure 4. Determination of gamma detection system time constant ($\tau = 1.94$ μs) using the model $I = I_{obs}/(1 - \tau I_{obs})$, where I is the actual count rate and I_{obs} is the measured count rate, for two sets of collimators (i.e. incident radiation intensity levels): (a) 3.175 mm and (b) 6.35 mm collimators on both source and detector.

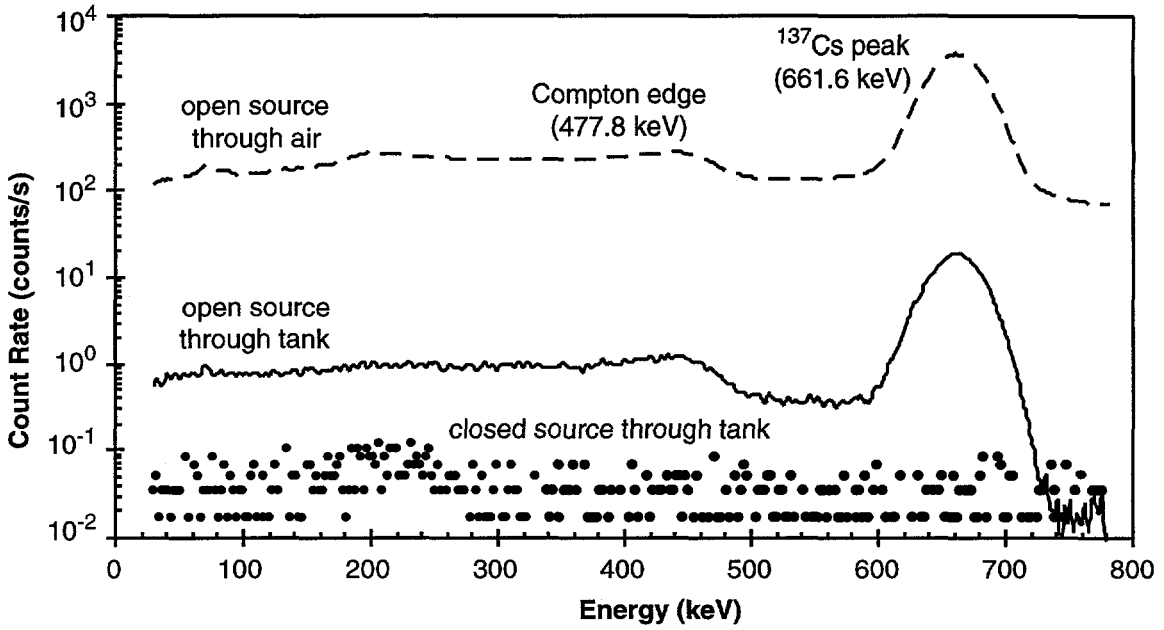

Figure 5. Energy spectrum of gamma detection system for an open source, with and without the test section present, and for a closed source.

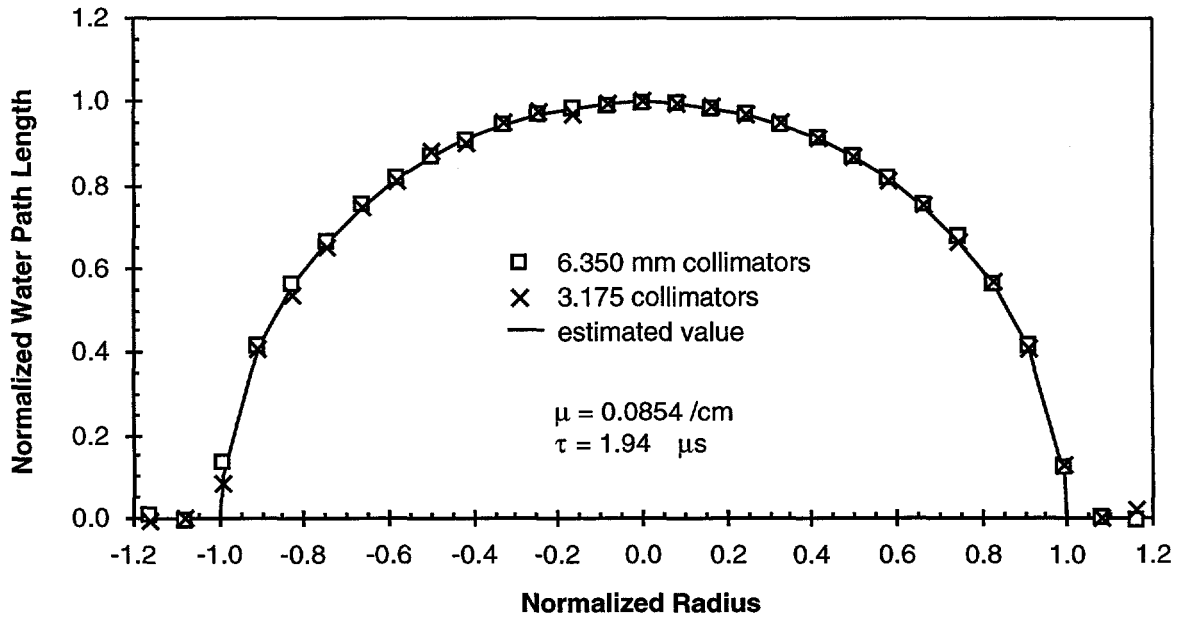

Figure 6. Calibration test for stainless steel bubble column: comparison of path length through water calculated using the measured transmission ratio (I/I_0) for full and empty scans versus horizontal scan location.

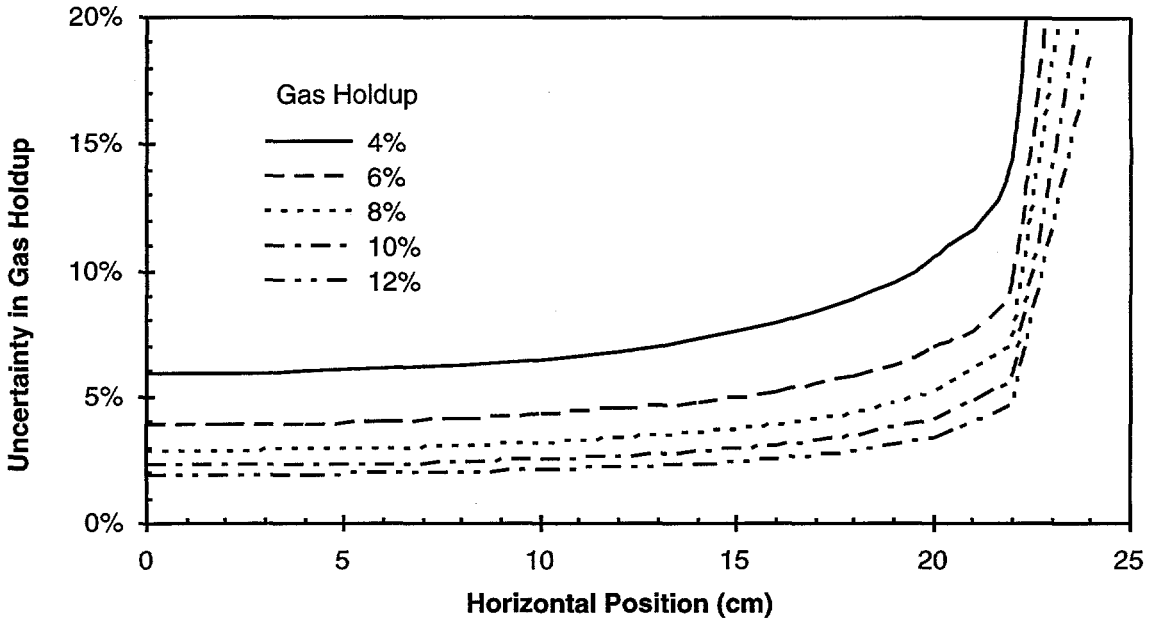

Figure 7. Uncertainty in gas holdup as a function of horizontal location and measured gas holdup for the 0.48 m stainless steel bubble column where a total of 20,000 counts are observed at each location.

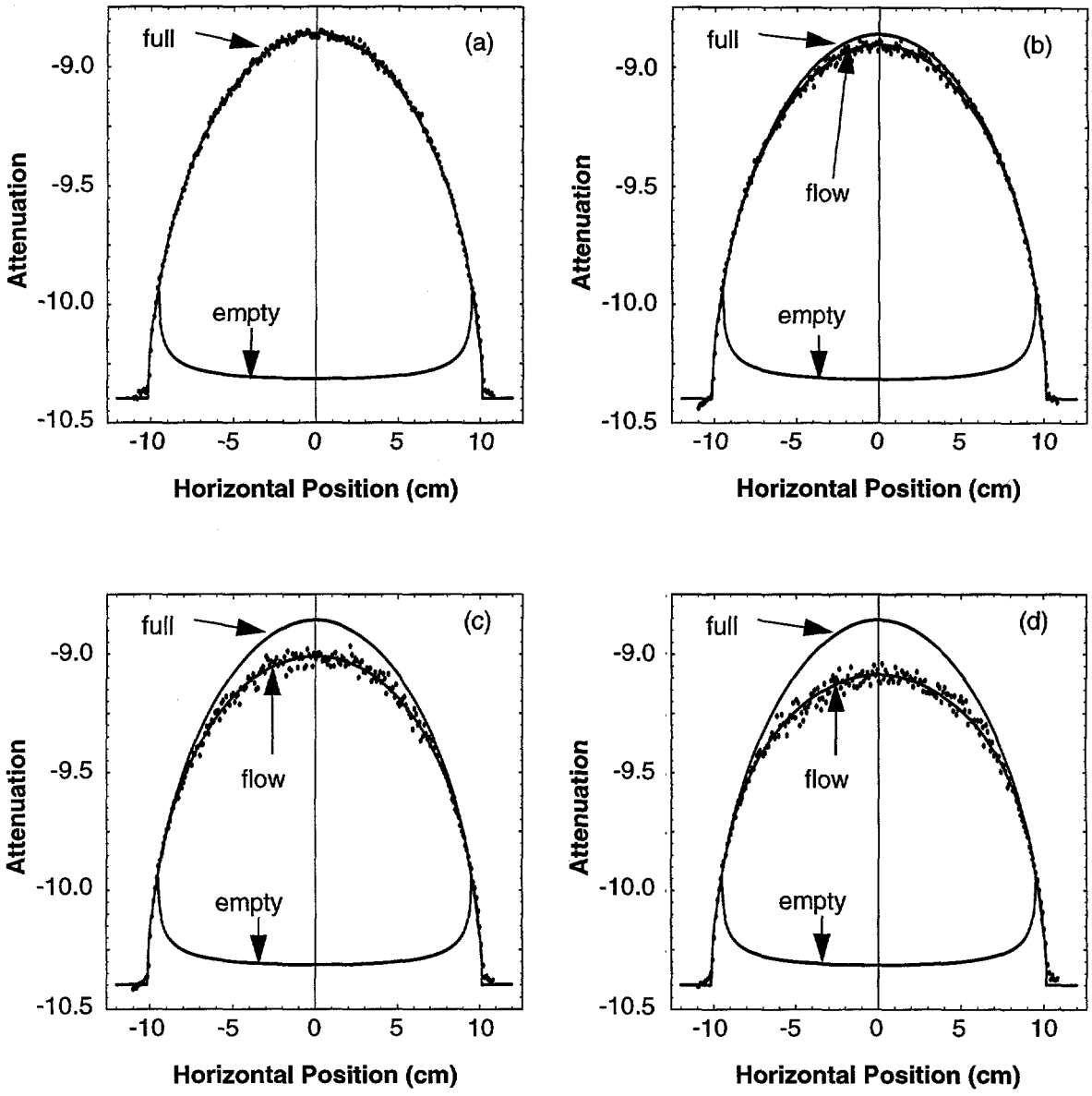

Figure 8. Gamma densitometry tomography results: air/water flow at STP, 0.19 m ID Lucite column, bubble cap gas sparger. "Full" is 100% water, "empty" is 100% air. Superficial gas velocity: (a) 0 (no air flow), 0% average gas holdup (b) 0.0147 m/s, average gas holdup 2.4%, (c) 0.0588 m/s, average gas holdup 8.2%, (d) 0.1176 m/s, average gas holdup 12.6%. Average gas holdup is based on axisymmetric tomographic reconstruction of data fit.

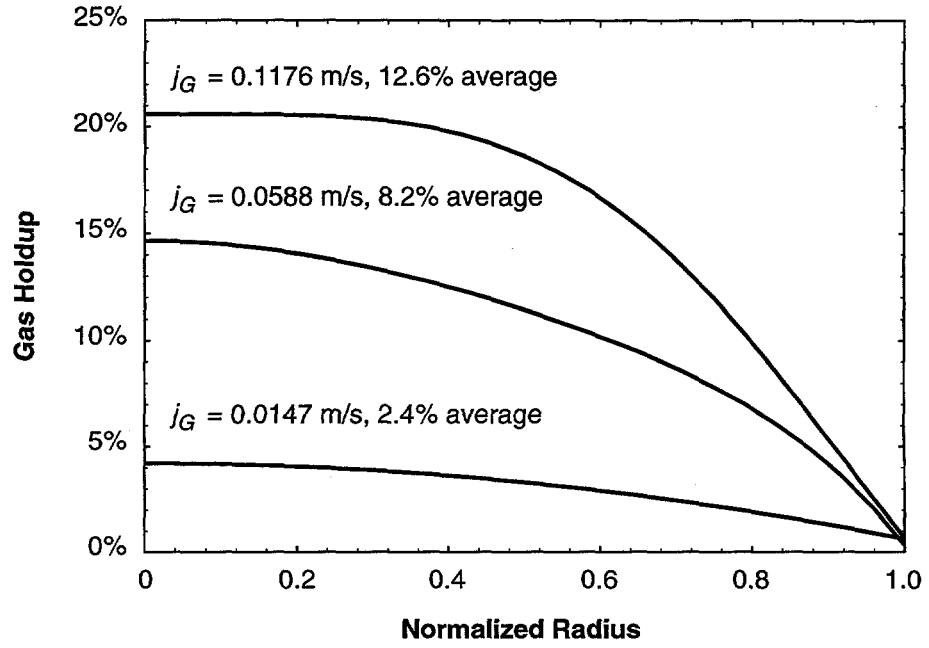

Figure 9. GDT-measured radial distributions of gas holdup, $f(r,R)$, as a function of superficial gas velocity (j_G) for air/water flow at ambient pressure and temperature in the 0.19 m ID Lucite column at a measurement location of $z/D = 3$ above a bubble cap sparger.

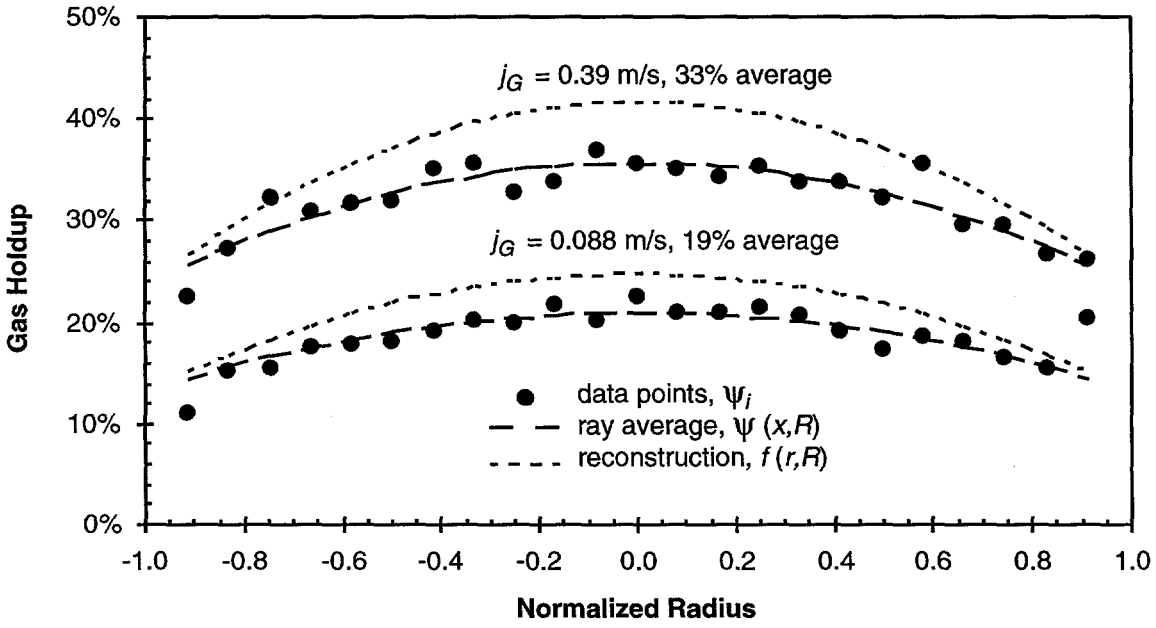

Figure 10. GDT-measured radial distributions of gas holdup as a function of superficial gas velocity (j_G) for air/water flow at ambient pressure and temperature in a 0.48 m ID stainless steel vessel at a measurement location of $z/D = 2$ above a ring type sparger.